Neuropsychologia 227 (2026) 109450

Contents lists available at ScienceDirect

Neuropsychologia

journal homepage: www.elsevier.com/locate/neuropsychologia

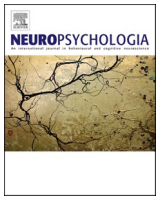

Tactile distance adaptation produces a coherent deformation of tactile space

Matthew R. Longo [a,*], Francesca Frisco [b], Elena Azañón [c,d,e,f,g]

[a] School of Psychological Sciences, Birkbeck, University of London, UK
[b] Department of Psychology, University of Milano-Bicocca, Italy
[c] Faculty of Psychology, Otto-von-Guericke University, Germany
[d] Leibniz Institute for Neurobiology, Magdeburg, Germany
[e] Department of Neurology, Faculty of Medicine, Otto-von-Guericke University, Germany
[f] Center for Behavioral Brain Sciences, Magdeburg, Germany
[g] Center for Intervention and Research on Adaptive and Maladaptive Brain Circuits Underlying Mental Health, Jena-Magdeburg-Halle, Germany

A B S T R A C T

Tactile distance illusions reveal systematic anisotropies in perceived spatial extent across the skin, such that distances oriented across the medio-lateral axis of the body are perceived as larger than those oriented along the proximo-distal axis. However, it remains unclear how these distortions are modified by the recent history of tactile stimulation. In the present study, participants judged the perceived distance between two touches on the dorsum of the hand across eight orientations, both before and after adaptation to a large tactile distance aligned with the medio-lateral axis. We applied the sinusoidal model of Fiori and Longo (2018) to characterise the geometric properties of tactile space and to quantify how they changed following adaptation. Adaptation produced a global reduction in perceived distance and a selective attenuation of anisotropy while preserving the orientation of maximal stretch. The aftereffects followed a sinusoidal tuning centred on the adapting orientation. Overall, our results indicate that somatosensory representations can adjust to recent stimulation without compromising their underlying spatial organisation, consistent with modulation at the level of population-based representations in somatosensory cortex.

1. Introduction

Illusions of the perceived distances between two touches have provided rich insight into spatial perception in the sense of touch (Longo, 2022, 2025). In the *tau effect*, for example, three sequential touches occur at equal spatial intervals, but unequal temporal intervals. Despite identical separation, the pair of touches separated by a longer time interval is perceived as being farther apart. Helson (1930) interpreted this phenomenon as a psychological analogue of Einsteinian 4-dimensional space-time, in which spatial and temporal information are integrated rather than processed independently. Weber (1834) described a different illusion in which the perceived distance between two touches increased as the stimulus was moved from a region of low spatial sensitivity (e.g., the forearm) to a region of higher sensitivity (e.g., the palm). This effect, known as *Weber's illusion*, has been widely replicated in subsequent research (e.g., Anema et al., 2008; Cholewiak, 1999; Goudge, 1918; Miller et al., 2016; Taylor-Clarke et al., 2004) and indicates a general relationship between perceived tactile distance and spatial sensitivity.

Other research has described illusions analogous to Weber's illusion on single skin surfaces as a function of orientation. Such *anisotropies* of perceived tactile distance have been described on many parts of the body, including the hand dorsum (Longo, 2017; Longo and Golubova, 2017; Longo and Haggard, 2011), the palm (Longo, 2020), the forearm (Chang and Longo, 2022; Green, 1982; Knight et al., 2014), upper arm (Chang and Longo, 2022), foot (Manser-Smith et al., 2021), shin (Stone et al., 2018), thigh (Green, 1982; Tosi and Romano, 2020), forehead (Fiori and Longo, 2018; Longo et al., 2015, 2020), cheek (Longo et al., 2020), and tongue (Chalmers and Longo, 2025). While the magnitude of anisotropy varies across the body, in general, there is a strikingly consistent tendency for distances oriented across the width of the body to be perceived as larger than distances oriented along the length of the body.

Fiori and Longo (2018) developed a computational model of these tactile distance anisotropies based on the hypothesis that they reflect a geometrically simple deformation of tactile space. The model was based on the idea that if tactile distance anisotropy reflects a simple stretch of tactile space along a single axis, this should produce predictable effects

This article is part of a special issue entitled: Neural basis of illusions published in Neuropsychologia.

* Corresponding author. Matthew Longo School of Psychological Sciences Birkbeck, University of London Malet Street, London, WC1E 7HX, UK.
E-mail address: m.longo@bbk.ac.uk (M.R. Longo).

https://doi.org/10.1016/j.neuropsychologia.2026.109450
Received 22 December 2025; Received in revised form 22 February 2026; Accepted 10 April 2026
Available online 12 April 2026

on perceived distance as a function of orientation. They showed that their three-parameter sinusoidal model provided a good fit to tactile distance judgments on multiple skin regions. They interpreted these results as evidence that tactile distance illusions reflect a simple and geometrically coherent stretch of tactile space.

Here, we extend this approach by examining whether tactile distance adaptation alters this geometric organisation of tactile space. Adaptation, in which prolonged exposure to one type of stimulus produces systematic alterations in the perception of subsequently presented stimuli, provides a particularly suitable method for this purpose, as it can reveal how recent sensory experience reshapes spatial representations. Adaptation aftereffects in touch have been reported for several forms of spatial information in touch, including location (Day and Singer, 1964; Li et al., 2017), curvature (van der Horst et al., 2008a; van der Horst et al., 2008b), size (Frisco et al., 2023, 2025; Hidaka et al., 2024; Maravita, 1997; Uccelli et al., 2019; Uznadze, 1966), orientation (Hidaka et al., 2022; Silver, 1969), and most relevant to the present context, perception of tactile distances (Calzolari et al., 2017; Hidaka et al., 2020; Tamè et al., 2026). Adaptation aftereffects thus appear to be widespread in spatial tactile perception.

In vision, adaptation aftereffects have been termed "the psychologist's microelectrode" (Frisby and Stone, 2010, pg. 75) on account of the revealing window they provide into the neurocognitive mechanisms underlying perceptual function. The same may be true for understanding tactile distance perception. In their initial report of tactile distance aftereffects, Calzolari and colleagues (2017) reported that the aftereffects are orientation specific. In an adaptation phase, tactile distances were repeatedly presented to each hand dorsum, a large (4 cm) distance to one hand and a small (2 cm) distance to the other. In a subsequent test phase, one tactile distance was applied to each hand and participants made two-alternative forced-choice (2AFC) judgments of which distance felt larger. The results showed a classic contrastive adaptation aftereffect: at test, there was a strong bias for tactile distances to feel smaller on the hand that had been adapted to the large distance. Such aftereffects were present both when adapting and test stimuli were presented in the medio-lateral hand axis (Exp 1) and in the proximo-distal hand axis (Exp 2). Critically, however, when the stimuli in the test phase were in a *different* orientation to those in the adaptation phase, the aftereffect disappeared. This orientation-specificity of adaptation mirrors results in visual adaptation aftereffects to size (Blakemore and Campbell, 1969; Blakemore and Sutton, 1969) and is consistent with adaptation being mediated by populations of neurons in early somatosensory cortices, which are known to show orientation-selective tuning functions (e.g., Bensmaia et al., 2008; Blakemore and Sutton, 1969; Fitzgerald et al., 2006; Hsiao et al., 2002; Thakur et al., 2006). Converging evidence comes from a recent study examining cross-category adaptation between tactile distance and texture (Jeschke et al., 2025). In this study, adaptation to a fixed tactile distance at the fingertips transferred to subsequently presented textures, such that textures with inter-indentation distances smaller than the adapting distance were perceived as less rough. Importantly, this transfer of aftereffects was observed only when the adapting distance and its orientation matched those of the test stimuli. No transfer was found when the adapting distance was oriented orthogonally to the inter-indentation direction of the texture stimulus, or when adaptation consisted of a single dot.

Traditionally, adaptation aftereffects were interpreted in terms of fatigue of individual, stimulus-selective neurons in the sensory pathways (e.g., Barlow and Hill, 1963). More recent interpretations, in contrast, have emphasized that adaptation produces more complex and subtle effects than can be explained by simple fatigue, suggesting that adaptation produces sophisticated adjustments to sensory representations to reflect the characteristics of recent experience (Solomon and Kohn, 2014). An elegant example was provided by Benucci and colleagues (2013) who measured the response of populations of orientation-selective neurons in primary visual cortex (V1) of cats following adaptation to specific orientations. Changes were found not only in specific neurons with preferred-orientations similar to the adapting stimulus, but more systematic changes across the entire population. Benucci and colleagues suggested that adaptation modulates population-level responses so as to maintain "population homeostasis" within the population.

Despite strong evidence that tactile distance adaptation is orientation-specific and likely originates in early somatosensory processing, it remains unknown how such adaptation alters the structure of tactile space as a whole. Prior studies have focused on a small number of orientations (i.e., across and along the axis of the hand or finger; i.e., 0° vs 90°), leaving open whether adaptation effects are confined to a specific axis or whether they produce systematic distortions across orientations. Moreover, no study has examined whether tactile distance adaptation interacts with the anisotropic geometry of tactile space described by the computational model of Fiori and Longo (2018).

In the present study, we addressed this gap by combining tactile distance adaptation with model-based analysis of tactile space. Participants made verbal judgments of the perceived distance between pairs of touches applied to the dorsum of the left hand in eight different orientations, both before and after adaptation to a large tactile distance in the medio-lateral orientation. By fitting the sinusoidal model of Fiori and Longo (2018) to each condition, we quantified how adaptation influences the global organization of tactile space. This approach allows us to determine whether adaptation produces a localized change confined to the adapted orientation or whether it induces a broader reorganization of tactile space that affects multiple orientations. If adaptation only affects the adapted axis, this would suggest a narrow, orientation-specific process. In contrast, if adaptation alters perceived distances across orientations, this would support the view that adaptation modulates population-level representations in somatosensory cortex, consistent with mechanisms that alter orientation tuning functions rather than a simple orientation-specific process.

2. Method

2.1. Participants

Twenty members of the Birkbeck community (11 women, 9 men), between 20 and 50 years of age (*M*: 26.3 years, *SD*: 7.6), participated for payment or course credit. All participants but two were right-handed as assessed by the Edinburgh Handedness Inventory (Oldfield, 1971) (*M*: 73.3, *SD*: 50.5). Testing began on one additional participant, who withdrew after only a few trials, and so was excluded from analyses. Procedures were approved by School of Psychological Sciences Research Ethics Committee at Birkbeck.

We aimed to have sufficient power to assess anisotropy using the paradigm of Fiori and Longo (2018) and also to measure the effects of tactile distance adaptation aftereffects, and so selected a sample size of 20 participants. This sample size was determined in advance of data collection and no interim analyses were conducted. Analyses were only performed after the full sample had been collected. In terms of tactile distance aftereffects, the effect size for the key *t*-test assessing aftereffects in the study of Calzolari and colleagues (2017) was $d_z = 2.44$ in Experiment 1 and $d_z = 1.59$ in Experiment 2. A power analysis using the smaller of these estimates in G*Power 3.1 (Faul et al., 2007) with alpha of .05 and power of .95 indicated that 8 participants were needed. In terms of measuring anisotropy, the main one-sample *t*-test assessing anisotropy in Fiori and Longo (2018) was $d = 1.74$. A power analysis in G*Power with alpha of .05 and power of .95 indicated that 7 participants were needed. Thus, our sample size of 20 is sufficient from both of these perspectives.

2.2. Stimuli

A set of eight lines was marked on the dorsum of the participant's left hand using a plastic stencil to define the eight different orientations

(from 0° to 157.5°). The 90° orientation was placed on the line connecting the centre of the wrist to the knuckle (metacarpophalangeal joint) of the middle finger. The other orientations were spaced at intervals of 22.5°, forming a compass rose, as shown in the left panel of Fig. 1. The lines indicating the different orientations intersected approximately in the centre of the hand dorsum. Participants were blindfolded during the experiment and were not allowed to see the lines drawn on their hand until the end of the experiment.

The stimuli were wooden cuticle sticks (Superdrug, London, UK) mounted in foamboard at different distances apart, as in many previous studies in our lab (e.g., Calzolari et al., 2017; Hidaka et al., 2020). The sticks tapered to a point around 1 mm in diameter. There were five distances: 20, 25, 30, 35, and 40 mm. The 40 mm stimulus was used only as an adapting stimulus, and the other stimuli were used as test stimuli. Stimuli were applied manually by an experimenter with moderate pressure for approximately 1 s on one of the lines. The experimenter practiced to try to maintain pressure as constant as possible across trials. Nevertheless, some trial-to-trial variability in pressure is inevitable with manual stimulation. Such variability, however, is unlikely to account for adaptation aftereffects, as it should not differ systematically across orientations or phases of the experiment. The exact location of stimuli on each line was jittered across trials to avoid repeated stimulation of the exact same skin locations. Participants were allowed to see the 30 mm stimulus at the start of the study to familiarize them with the nature of the stimuli, but were not shown the other stimuli and were not told how many stimuli there were.

2.3. Procedures

The task was identical to that used by Fiori and Longo (2018). Participants made unspeeded verbal judgments of the perceived distance between the two touched points by giving a number in cm. Participants were allowed to respond using inches if they were more comfortable with that unit, but all participants chose to respond using cm. They were encouraged to be as precise as possible, and to consider using decimal responses (e.g., “3.2 cm”, rather than just “3 cm”). Participants were allowed to give a response of “0 cm” if they felt only a single touch.

There were two experimental conditions, *baseline* and *adaptation*. The baseline condition was similar to Fiori and Longo (2018). On each trial, a single touch was applied, and the participant made a verbal response. In the adaptation condition, the test stimulus was preceded by a 4 cm adapting stimulus applied at the 0° orientation (i.e., a stimulus aligned with the medio-lateral hand axis). The adaptation procedures were similar to those used in our previous study (Calzolari et al., 2017). On the first adaptation trial of each block, 60 s of adaptation (consisting of about 60 touches) was applied, and an additional 10 s of “top up” adaptation was applied at the start of each subsequent trial. Adaptation consisted of repeated presentation of the 4 cm stimulus for approximately 1 s at a time (including indentation and release) at different locations along the 0° line. This means that stimulation was not systematically applied to the same skin locations, which should produce spatial summation across the range of skin locations stimulated (Gescheider et al., 2005; Reid et al., 2015).

There were two blocks of each condition, counterbalanced across participants in ABBA fashion, with the first condition (baseline or adaptation) counterbalanced across participants. Each block consisted of two repetitions of each of the four test stimuli (i.e., 20, 25, 30, and 35 mm) at each of the eight orientations, in random order. There were thus 128 trials of each condition, and 256 trials in total. Participants were allowed to take a short break between blocks to rest and to allow the effects of adaptation to dissipate.

2.4. Analysis

The analysis was similar to previous studies using this paradigm (Fiori and Longo, 2018; Mainka et al., 2021). The judgment on each trial was expressed as a proportion of actual size and the average was calculated for each orientation in each condition. While it was necessary to vary stimulus size across trials so that participants could not just give the same response on each trial, this was not a variable of theoretical interest in this study. The four stimulus sizes were therefore collapsed, consistent with previous studies using this paradigm (Fiori and Longo, 2018; Mainka et al., 2021). We used a repeated-measures analysis of variance (ANOVA) to investigate the effects of orientation and condition (baseline, adaptation) with stimulus distance (i.e., 2, 2.5, 3, and 3.5 cm) also included as a factor for completeness. Where Mauchley's test indicated a violation of the sphericity assumption, the Greenhouse-Geisser correction was applied. Partial eta-squared (η_p^2) was used as a measure of effect size. To assess whether adaptation affected response variability, we compared the standard deviation of judgments between baseline and adaptation conditions across orientations using a paired *t*-test.

We next applied the computational model developed by Fiori and Longo (2018) to quantify how perceived tactile distance varies with stimulus orientation. The logic of this model is to think of stretch of

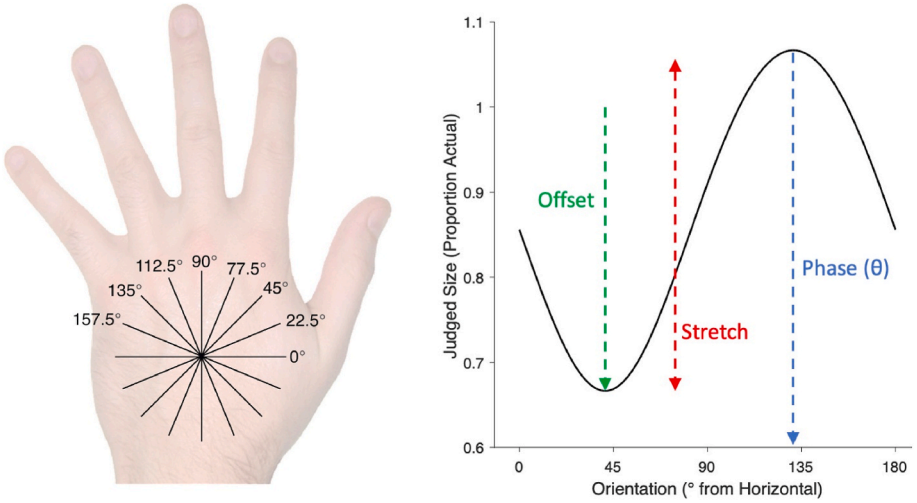

Fig. 1. *Left panel*: The eight stimulus orientations used in the study. On each trial, a tactile distance was applied in one orientation and the participant judged how far apart the two touches were. *Right panel*: Responses were modelled as a sinusoidal function of stimulus orientation with three parameters: (1) the *phase* (blue) controls the orientation of the peak of the sinusoid, that is the axis of maximal stretch; (2) the *stretch* (red)controls the amplitude of the sinusoid, that is the magnitude of tactile distance anisotropy; and (3) the *offset* (green) controls the perceived size at the trough of the sinusoid.

tactile space as being applied along a specific axis on the skin (controlled by a *phase* parameter). Each distance is decomposed into its components parallel to this axis of maximal stretch (i.e., the cosine component) and the orthogonal orientation (i.e., the sine component). Perceived distance can be estimated from these components using the Pythagorean theorem. The model thus applies a *stretch* parameter to the cosine component. Finally, an *offset* parameter was included to translate the entire curve up and down to reflect overall biases to overestimate or underestimate perceived distances. Thus, the overall model is:

$$Predicted\ distance = offset + \sqrt{(stretch \times \cos(\Theta - phase))^2 + \sin(\Theta - phase)^2}$$

The resulting model is a sinusoid, as shown in the right panel of Fig. 1. The *stretch* parameter controls the amplitude of the sinusoid, that is the amount by which judgments differ for stimuli in the orientation of maximal stretch and stimuli in the orthogonal orientation, as shown by the red line in the plot. The *phase* parameter controls the orientation of maximal stretch, that is the stimulus orientation aligned with the peak of the sinusoid, as shown by the blue line in the plot. Finally, the *offset* parameter indicates the perceived size at the trough of the sinusoid. That is, it translates the sinusoid up or down depending on overall levels of over- or under-estimation.

For each participant, we calculated best-fitting sinusoids for both the baseline and adaptation condition using the *fminsearch* function in MATLAB (Mathworks, Natick, MA) which uses the Nelder-Mead method to identify the set of parameters which minimized the sum of squared deviations between the modelled sinusoid and the actual data. In each case, we extracted the three parameters of the model and the R^2 value, quantifying the proportion of variance in the data that is accounted for by the model.

To investigate the presence of tactile distance anisotropy in each condition, we calculated the ratio of the fitted values of the model as orientations of 0° (i.e., aligned with the medio-lateral hand axis) and 90° (i.e., aligned with the proximo-distal hand axis). A one-sample *t*-test was used to compare the mean ratio in each condition to a ratio of 1. A paired *t*-test was used to compare the magnitude of anisotropy in the two conditions. (Note that for this and other tests involving ratios, data were log-transformed for statistical tests and calculation of means. Mean values were converted back to a ratio for reporting.) As measures of effect size, we used Cohen's *d* for one-sample *t*-tests and Cohen's d_z for paired *t*-tests.

Paired *t*-tests were used to compare the values of the stretch and offset parameters between the two conditions. Because the phase parameter is an angle, a different approach is required to analyse it. To assess whether the orientation of maximal stretch was consistent across participants, we conducted a Rayleigh test, which tests the null hypothesis that a set of angles are uniformly distributed around the circle (Batschelet, 1981) using the *CircStat* toolbox for MATLAB (Berens, 2009). Separate Rayleigh tests were conducted for each condition. The effect of adaptation was assessed by using a one-sample test against 0° on the mean angle on the angular difference between the adaptation and baseline conditions, to test whether adaptation produced a systematic change in phase compared to baseline.

Raw data and analysis scripts are available on the Open Science Framework: https://osf.io/evyq2/.

3. Results

The results are shown in the left panel of Fig. 2. An ANOVA revealed a significant main effect of orientation, $F(2.94, 55.77) = 10.83$, $p < .001$, $\eta_p^2 = .363$, consistent with the presence of tactile distance anisotropy. There was also a significant main effect of condition, $F(1, 19) = 45.06$, $p < .0001$, $\eta_p^2 = .703$, indicating that adaptation modulated responses. Most importantly, there was a significant interaction of orientation and condition, $F(7, 133) = 7.05$, $p < .001$, $\eta_p^2 = .271$, indicating that the effect of adaptation differed systematically as a function of orientation. There were also significant effects involving stimulus distance, including a main effect of distance, $F(1.14, 21.69) = 6.43$, $p < .001$, $\eta_p^2 = .253$; an interaction between distance and condition, $F(1.72, 32.66) = 9.70$, $p < .0001$, $\eta_p^2 = .338$; an interaction between distance and orientation, $F(21, 399) = 1.96$, $p < .01$, $\eta_p^2 = .094$; and a three-way interaction, $F(21, 399) = 1.82$, $p < .02$, $\eta_p^2 = .087$. The inclusion of distance was exploratory and not part of our a priori planned analyses. We will therefore focus on our planned analyses of the condition by adaptation interaction before returning to a more exploratory analysis of distance.

Separate ANOVAs in each condition showed significant effects of orientation both in the baseline condition, $F(3.41, 64.83) = 17.08$, $p < .0001$, $\eta_p^2 = .473$, and in the adaptation condition, $F(3.29, 62.51) = 3.22$, $p < .05$, $\eta_p^2 = .145$. Holm–Bonferroni–corrected pairwise *t*-tests between the two conditions at each orientations showed significant differences at all orientations (all *t*'s > 2.47).

The curves in the left panel of Fig. 2 show the best-fitting sinusoids fit to the grand-mean data from the baseline condition (blue) and adaptation condition (orange). We first investigated the results from the baseline condition. Overall, the model showed good fit to the data ($R^2 = .970$). Data from individual participants was also well fit, with a mean R^2 of .660 (*SD*: .240, range: .067-.924).

The blue vertical line in the left panel of Fig. 2 shows the peak of the sinusoidal model, that is the stimulus orientation for which tactile distances are perceived as largest. The same data is depicted in a different way in the left panel of Fig. 3. The Rayleigh test provided clear evidence against the phases of the model being randomly distributed, $z = 15.78$, $p < .0001$. The orientation of maximum stretch was near to a medio-

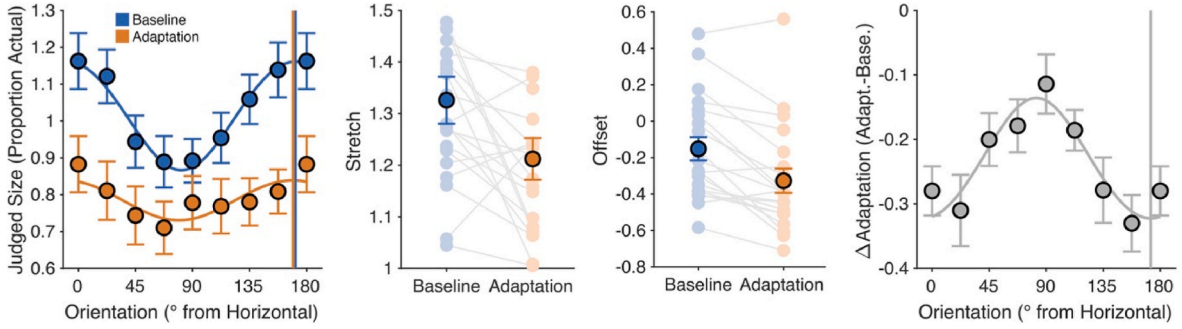

Fig. 2. Experimental results. *Left panel*: judged size as a function of stimulus orientation in the baseline condition (blue) and the adaptation condition (orange). The curves show best-fitting sinusoidal functions. The vertical lines indicate the peak of the sinusoids (i.e., the axis in which tactile space is stretched). Error bars are one standard error. For illustrative purposes, the same data point is shown as both 0° and 180°, but was only included once in analyses. *Centre panels*: values of the stretch and offset parameters in the two conditions. Dark data points are grand means and light data points are individual participant data. *Right panel*: The effect of adaptation as a function of orientation (i.e., adaptation - baseline). The curve is the difference between the two sinusoids.

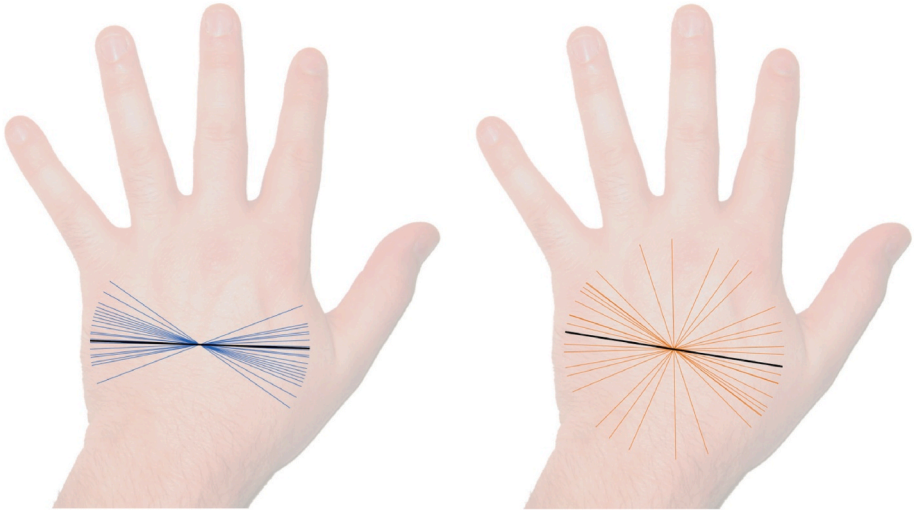

Fig. 3. The axis of maximal stretch in the baseline condition (left panel, blue) and the adaptation condition (right panel, orange). Each thin coloured line indicates the axis of maximal stretch (i.e., the orientation of the peak of the sinusoidal model) for a single participant. The black line indicates the circular mean across participants.

lateral stimulus oriented across the width of the hand, consistent with known anisotropies, as discussed above. To quantify anisotropy, we compared the ratio of fitted values of the model for stimuli aligned with the medio-lateral hand axis (0°) and the proximo-distal axis (90°). The mean ratio was 1.33, significantly greater than 1, $t(19) = 7.18$, $p < .0001$, $d = 1.606$. Overall, these results provide a clear replication of the main findings of the study of Fiori and Longo (2018).

In the adaptation condition, the model showed decent overall fit to the data ($R^2 = .640$). The fit to individual participant data had a mean R^2 of .464 (*SD*: .284, range: .003-.916). R^2 values were significantly lower in the adaptation than in the baseline condition, $t(19) = 3.06$, $p < .01$, $d_z = .685$. This difference in model fit is expected given that adaptation clearly reduced the amplitude of the best-fitting sinusoid, which naturally reduces the signal-to-noise ratio of the model. It is also possible that adaptation could increase the inter-participant or inter-trial variability. However, there was no evidence that variability as such was larger following adaptation. Across the eight orientations, the mean standard deviation of judgments was similar at baseline and after adaptation (.312 vs. .322), and did not differ statistically, $t(7) = .75$, $p = .462$. This suggests that the reduced model fit in the adaptation condition reflects the reduced amplitude of the orientation-dependent pattern, rather than increased variability in the data.

The orange vertical line in the left panel of Fig. 2 and the right panel of Fig. 3 show the orientation of maximum stretch in the adaptation condition. While there was clearly greater variability across participants than in the baseline condition, the Rayleigh test showed that the phase of the model was not randomly distributed, $z = 3.24$, $p < .05$. As is clear from both figures, the average orientation of maximum stretch was highly similar in the two conditions. As in the baseline condition, we calculated anisotropy by taking the ratio of fitted values at 0° and 90°, which was again above 1 (*M*: 1.148), but did not quite reach statistical significance, $t(19) = 2.08$, $p = .0515$, $d = .465$. The magnitude of anisotropy was significantly reduced in the adaptation condition compared to baseline, $t(19) = 3.26$, $p < .005$, $d_z = .728$.

We next directly compared the parameters of the model in the two conditions to determine the effects of adaptation. To compare the phase of the models, we first calculated the angular deviation of the phase in the adaptation condition to the baseline condition. A circular one-sample test for mean angle provided no evidence that this deviation differed from 0°, $z = .28$, *n.s.*

In contrast, there was clear evidence that adaptation modulated the other two parameters of the model, as shown in the middle two panels of Fig. 1. The stretch parameter was significantly reduced following adaptation (*M*: 1.21, *SD*: .18) compared to baseline (*M*: 1.33, *SD*: .20), $t(19) = 3.28$, $p < .005$, $d_z = .734$, indicating that adaptation reduced the amplitude of the sinusoid, consistent with the analysis above showing reduced anisotropy following adaptation. There was also a significant reduction in the offset parameter following adaptation (*M*: −.33, *SD*: .30) compared to baseline (*M*: −.15, *SD*: .29), $t(19) = 4.88$, $p < .0001$, $d_z = 1.092$, indicating that adaptation produced a general underestimation of tactile distances, translating the sinusoid down.

The right-most panel of Fig. 2 shows the difference between the adaptation and baseline conditions for each orientation. The curve reflects the difference between the sinusoidal models fit to each condition (i.e., the difference between the orange and blue curves in the left panel). The significant interaction in the ANOVA reported above indicated that the magnitude of adaptation differed systematically as a function of orientation. This figure shows that the adaptation itself shows a sinusoidal tuning function.

Finally, given the significant three-way interaction of condition, orientation, and distance reported above, we conducted exploratory analyses breaking the results down separately by each of the four distances. It is important to note that the study was not designed to address this issue, and these analyses involve very small numbers of trials at each orientation per distance bin, and so should be treated with caution.

Fig. 4 shows grand mean data with sinusoidal curves (top row) and adaptation tuning curves (bottom row) for each of the four stimulus distances. Notably, while there were clear effects of adaptation for the three smallest distances, the effect was reduced for the 3.5 cm stimulus, which is the closest test stimulus to the 4 cm adapting stimulus.

As above, we quantified anisotropy by comparing the ratio of fitted values of the model for stimuli aligned with the medio-lateral hand axis (0°) and the proximo-distal axis (90°). At baseline there was clear anisotropy for all four stimulus distances: 2 cm (*M*: 1.36), $t(19) = 4.43$, $p < .001$, $d = 1.016$; 2.5 cm (*M*: 1.27), $t(19) = 3.72$, $p < .002$, $d = .852$; 3 cm (*M*: 1.45), $t(19) = 7.36$, $p < .0001$, $d = 1.689$; and 3.5 cm (*M*: 1.32), $t(19) = 5.76$, $p < .0001$, $d = 1.322$. In striking contrast, after adaptation there remained a significant anisotropy for 3.5 cm stimuli (*M*: 1.37), $t(19) = 5.52$, $p < .0001$, $d = 1.267$, but there was no significant anisotropy for any of the three smaller distances: 2 cm (*M*: 1.07), $t(19) = .31$, $p = .758$. $d = .072$; 2.5 cm (*M*: 1.060), $t(19) = .57$, $p = .573$, $d = .131$; and 3 cm (*M*: 1.11), $t(19) = 1.41$, $p = .175$, $d = .323$.

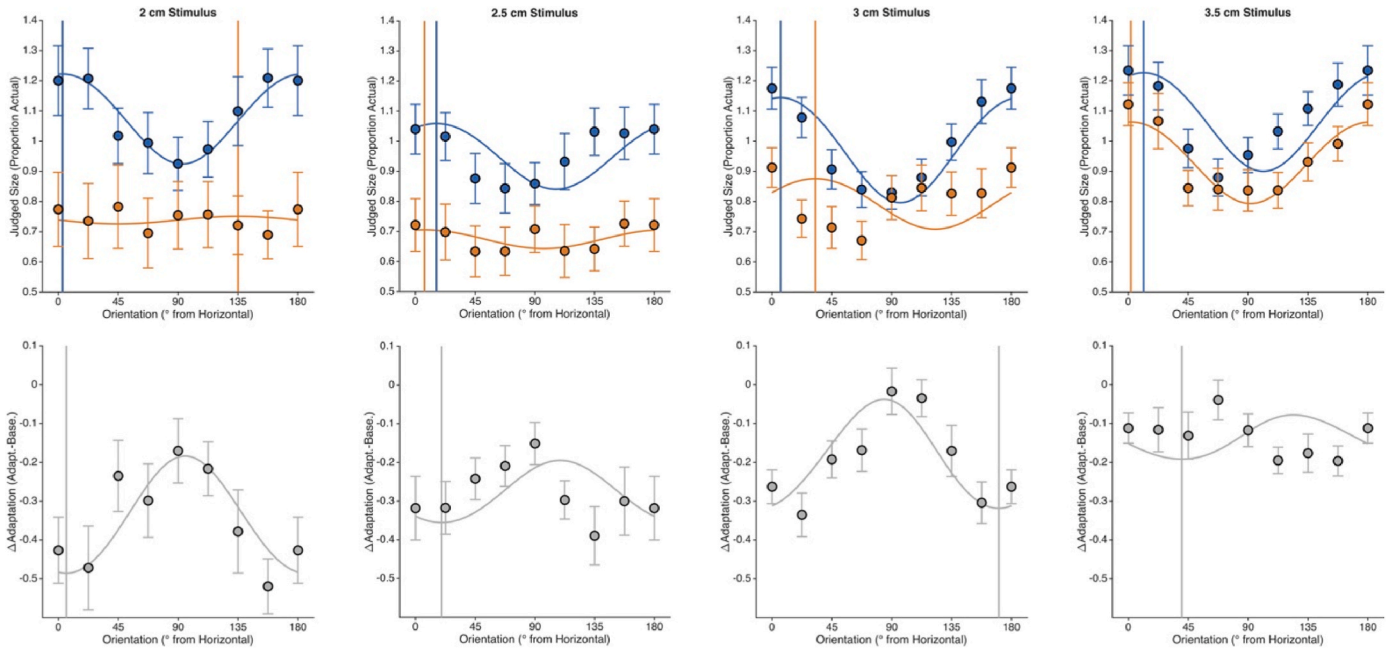

Fig. 4. Experimental results by stimulus distance. *Top row*: judged size as a function of stimulus orientation in the baseline condition (blue) and the adaptation condition (orange). The curves show best-fitting sinusoidal functions. The vertical lines indicate the peak of the sinusoids (i.e., the axis in which tactile space is stretched). Error bars are one standard error. *Bottom row*: The effect of adaptation as a function of orientation (i.e., adaptation - baseline). The curve is the difference between the two sinusoids.

4. Discussion

These results provide clear evidence for robust adaptation aftereffects for tactile distance, consistent with other recent studies (Calzolari et al., 2017; Hidaka et al., 2020; Tamè et al., 2026). In contrast to previous studies which used two-alternative forced-choice judgments and fit psychometric functions, we used a richer computational model of how perceived distance varies as a function of orientation (Fiori and Longo, 2018). Adaptation to a large tactile distance in the medio-lateral orientation produced clear alterations in the parameters of this model, showing: (1) an overall reduction of responses independent of orientation (indexed by the offset parameter), and (2) a specific reduction centred on the orientation of the adapting stimulus and showing a sinusoidal tuning function (indexed by the stretch parameter).

Previous studies showed that tactile distance aftereffects show orientation specificity (Calzolari et al., 2017). The precision of this specificity, however, was not clear. Because that study compared only two orientations, it was possible that adaptation affected only a narrow band immediately surrounding the orientation of the adapting stimulus. The present results, in contrast, show that adaptation has a wide, sinusoidal tuning function. This extends the findings of previous studies of tactile distance adaptation (Calzolari et al., 2017; Hidaka et al., 2020; Tamè et al., 2026) and provides important insight into the potential neuro-cognitive mechanisms underlying it.

Orientation-selective neurons in both S1 (e.g., Hsiao et al., 2002; Pubols and Leroy, 1977) and S2 (e.g., Fitzgerald et al., 2006; Thakur et al., 2006) feature Gaussian orientation tuning functions, with a single preferred orientation and progressively weaker responses for stimuli at different orientations. In the present behavioural results, we show an analogous tuning function for the effects of adaptation on perceived tactile distances. This result indicates that adaptation does not exclusively modulate responses of neurons with preferred orientations identical to the adapting stimulus, but instead is modulating larger-scale responses among the entire population of orientation-selective neurons.

The present results suggest that there are two distinct components of tactile distance adaptation. First, a global reduction in perceived distance, quantified by the offset parameter, indicating that all test stimuli are judged as shorter following adaptation. Second, there is an orientation-specific reduction, quantified by the stretch parameter, such that the aftereffect is strongest near the adapted orientation. The functional significance of these two components is not entirely clear. Notably, the global reduction was not found in our previous study on tactile distance aftereffects (Calzolari et al., 2017). In that paradigm, participants compared which of two touches felt larger. Any uniform rescaling of perceived distance affecting both stimuli equally would not alter their relative difference and would therefore remain undetected. These two effects of adaptation may reflect fundamentally different types of computational process. The general effect on the offset parameter could reflect a global recalibration of tactile scale (e.g., a shift in the expected scale of tactile distances based on recent sensory history), whereas the orientation-specific effect shown by changes in the stretch parameter could reflect feature specific recalibration (e.g., a change in the weighting or precision of an anisotropic prior, with its geometric structure preserved). These alterations can be viewed as reflections of Bayesian recalibration of sensory inputs, such as have been recently discussed in other domains of body representation (e.g., Bertoni et al., 2023; Martinelli et al., 2025).

In this sense, our results have an interesting connection to the results of Benucci and colleagues (2013) in cat visual cortex, who found that the effects of adaptation to specific visual orientations modulated the overall activation within the population of orientation-selective neurons such as to maintain “population homeostasis”. There were two main effects of adaptation that Benucci and colleagues identified: (1) an overall reduction of responses regardless of preferred-orientation, and (2) a larger reduction in responses specifically for neurons with preferred-orientations near the adapting stimulus. Remarkably, as different as the present study is from that of Benucci and colleagues, being a behavioural study of touch in humans, the effects of adaptation showed very similar effects. First, we found a clear effect of adaptation on the offset parameter of our model, reflecting an overall reduction of perceived size across orientations following adaptation. Second, we found a clear Gaussian tuning function for adaptation, quantified by the stretch parameter of the model, with the largest aftereffects at orientations similar to the adapting stimulus. While the present results are

completely behavioural, they have an intriguing resemblance to these neural findings. Thus, it is possible that tactile distance adaptation may modulate neural processing in somatosensory cortex so as to maintain population homeostasis, analogous to the findings in visual cortex by Benucci and colleagues. Behaviourally, this homeostasis can be described as adaptation maintaining the spatial coherence of tactile space, as quantified by Fiori and Longo (2018). Adaptation in the present study had the effect of reducing the magnitude of the baseline stretch in tactile space, but maintained the spatial coherence of tactile space.

In the present study, there was a clear tuning function of adaptation as a function of stimulus orientation, although participants made judgments of the distance between touches and orientation was completely irrelevant to their task. This contrasts with other studies, which have identified tactile *tilt aftereffects* in which judgments of orientation are modulated by adaptation to specific orientations (Hidaka et al., 2022; Silver, 1969). Both types of aftereffects may thus arise from common populations of orientation-selective neurons, which have been described both in S1 and S2. It is interesting to note in this context that tactile aftereffects for tilt and distance share several forms of stimulus specificity. Both tilt (Hidaka et al., 2022) and distance (Calzolari et al., 2017; Tamè et al., 2026) aftereffects transfer between two-point stimuli and continuous lines, fail to transfer between the right and left hands, and are defined in a hand-centred rather than an external reference frame. It will be interesting in future research to look more precisely at the relations between tactile tilt and distance aftereffects.

Exploratory analyses breaking our effects down by distance suggested that the effects of adaptation were smallest for test stimuli closest in distance to the 4 cm adapting stimulus and larger for more dissimilar test stimuli. While the present study was not designed to address this issue, and this effect remains tentative, it may have interesting links to mechanistic models of adaptation. In vision, many studies have used visual adaptation aftereffects to distinguish between *multichannel* models in which distinct pools of neurons code different values along a stimulus continuum, and *opponent-coding* models in which two broadly-tuned channels code for opposite poles of a stimulus continuum. In general, multichannel models predict that aftereffects should be largest for test stimuli similar to the adapting stimulus, whereas opponent-coding models predict that aftereffects should be larger the more different the test stimulus is from the adaptor. In different visual domains, studies have provided evidence for both types of model. Evidence for multichannel coding has been found for visual domains such as orientation (Clifford et al., 2000; Gibson and Radner, 1937) and spatial frequency (Blakemore and Sutton, 1969), while evidence for opponent-coding models has been found for colour (Webster and Leonard, 2008) and for face aftereffects of identity (Rhodes and Jeffery, 2006; Robbins et al., 2007), gender (Pond et al., 2013), and emotional expression (Burton et al., 2013; Rhodes et al., 2017; Hong and Yoon, 2018). The present results are consistent with the pattern that would be expected from an opponent-coding mechanism coding tactile distance. This will be an important topic to investigate further in future studies.

There are several limitations on the generalisability of the present findings. This study investigated only a single skin region (the dorsum of the left hand) and applied adaptation only in a single orientation (the medio-lateral hand axis). In our previous study (Calzolari et al., 2017), we showed that adaptation can occur for stimuli in both the medio-lateral and proximo-distal orientations. Nevertheless, the change in the magnitude of anisotropy measured in this study may have been linked to the fact that we presented adapting stimuli aligned with the medio-lateral axis, aligned with the anisotropy itself. We suspect that adapting stimuli applied in the proximo-distal axis would increase, rather than decrease anisotropy. Similarly, we believe that adaptation could also induce anisotropy orthogonal to the adapting stimulus on a skin region without any baseline anisotropy, such as the belly (cf., Longo et al., 2019). It would be interesting in future studies to investigate these hypotheses.

In summary, our findings show that tactile distance adaptation induces both global and orientation-tuned changes in perceived spatial extent, consistent with modulation at the level of population-based representations in somatosensory cortex. By applying a computational model to behaviour across multiple orientations, we demonstrate that adaptation alters the magnitude of tactile space while preserving its geometric coherence. These results clarify how somatosensory processing adapts to recent stimulation while preserving the overall organisation of tactile space, and they highlight parallels with population homeostasis observed in vision.

CRediT authorship contribution statement

Matthew R. Longo: Writing – original draft, Visualization, Supervision, Software, Project administration, Methodology, Formal analysis, Conceptualization. **Francesca Frisco:** Writing – review & editing, Investigation, Conceptualization. **Elena Azañón:** Writing – review & editing, Software, Formal analysis, Conceptualization.

References

Anema, H.A., Wolswijk, V.W.J., Ruis, C., Dijkerman, H.C., 2008. Grasping Weber's illusion: the effect of receptor density differences on grasping and matching. Cogn. Neuropsychol. 25, 951–967. https://doi.org/10.1080/02643290802041323.

Barlow, H.B., Hill, R.M., 1963. Evidence for a physiological explanation of the waterfall phenomenon and figural after-effects. Nature 200 (4913), 1345–1347. https://doi.org/10.1038/2001345a0.

Batschelet, E., 1981. Circular Statistics for Biology. Academic.

Bensmaia, S.J., Denchev, P.V., Dammann, J.F., Craig, J.C., Hsiao, S.S., 2008. The representation of stimulus orientation in the early stages of somatosensory processing. J. Neurosci. 28 (3), 776–786. https://doi.org/10.1523/JNEUROSCI.4162-07.2008.

Benucci, A., Saleem, A.B., Carandini, M., 2013. Adaptation maintains population homeostasis in primary visual cortex. Nat. Neurosci. 16 (6), 724–729. https://doi.org/10.1038/nn.3382.

Berens, P., 2009. CircStat: a MATLAB toolbox for circular statistics. J. Stat. Software 31 (10). https://doi.org/10.18637/jss.v031.i10.

Bertoni, T., Mastria, G., Akulenko, N., Perrin, H., Zbinden, B., Bassolino, M., Serino, A., 2023. The self and the Bayesian brain: testing probabilistic models of body ownership through a self-localization task. Cortex 167, 247–272. https://doi.org/10.1016/j.cortex.2023.06.019.

Blakemore, C., Campbell, F.W., 1969. On the existence of neurones in the human visual system selectively sensitive to the orientation and size of retinal images. J. Physiol. (Paris) 203 (1), 237–260. https://doi.org/10.1113/jphysiol.1969.sp008862.

Blakemore, C., Sutton, P., 1969. Size adaptation: a new aftereffect. Science 166 (3902), 245–247. https://doi.org/10.1126/science.166.3902.245.

Burton, N., Jeffery, L., Skinner, A.L., Benton, C.P., Rhodes, G., 2013. Nine-year-old children use norm-based coding to visually represent facial expression. J. Exp. Psychol. Hum. Percept. Perform. 39 (5), 1261–1269. https://doi.org/10.1037/a0031117.

Calzolari, E., Azañón, E., Danvers, M., Vallar, G., Longo, M.R., 2017. Adaptation aftereffects reveal that tactile distance is a basic somatosensory feature. Proc. Natl. Acad. Sci. 114 (17), 4555–4560. https://doi.org/10.1073/pnas.1614979114.

Chalmers, R., Longo, M.R., 2025. Tactile distance anisotropy on the tongue. Q. J. Exp. Psychol. https://doi.org/10.1177/17470218251330597.

Chang, K.-C., Longo, M.R., 2022. Similar tactile distance anisotropy across segments of the arm. Perception 51 (5), 300–312. https://doi.org/10.1177/03010066221088164.

Cholewiak, R.W., 1999. The perception of tactile distance: influences of body site, space, and time. Perception 28, 851–875. https://doi.org/10.1068/p2873.

Clifford, C.W., Wenderoth, P., Spehar, B., 2000. A functional angle on some after-effects in cortical vision. Proceedings of the Royal Society B 267 (1454), 1705–1710. https://doi.org/10.1098/rspb.2000.1198.

Day, R.H., Singer, G., 1964. A tactile spatial aftereffect. Aust. J. Psychol. 16 (1), 33–37. https://doi.org/10.1080/00049536408255500.

Faul, F., Erdfelder, E., Lang, A.-G., Buchner, A., 2007. G*Power 3: a flexible statistical power analysis program for the social, behavioral, and biomedical sciences. Behav. Res. Methods 39, 175–191. https://doi.org/10.3758/BF03193146.

Fiori, F., Longo, M.R., 2018. Tactile distance illusions reflect a coherent stretch of tactile space. Proc. Natl. Acad. Sci. 115, 1238–1243. https://doi.org/10.1073/pnas.1715123115.

Fitzgerald, P.J., Lane, J.W., Thakur, P.H., Hsiao, S.S., 2006. Receptive field properties of the macaque second somatosensory cortex: representation of orientation on different finger pads. J. Neurosci. 26 (24), 6473–6484. https://doi.org/10.1523/JNEUROSCI.5057-05.2006.

Frisby, J.P., Stone, J.V., 2010. Seeing: the Computational Approach to Biological Vision, 2nd Ed. MIT Press.

Frisco, F., Daneyko, O., Maravita, A., Zavagno, D., 2023. The influence of arm posture on the Uznadze haptic aftereffect. J. Exp. Psychol. Hum. Percept. Perform. 49 (9), 1271–1279. https://doi.org/10.1037/xhp0001144.

Frisco, F., Zavagno, D., Maravita, A., 2025. Hands-on adaptation: bodily stimuli increase size adaptation aftereffect. J. Exp. Psychol. Hum. Percept. Perform. 51 (6), 721–731. https://doi.org/10.1037/xhp0001294.
Gescheider, G.A., Güçlü, B., Sexton, J.L., Karalunas, S., Fontana, A., 2005. Spatial summation in the tactile sensory system: probability summation and neural integration. SMR (Somatosens. Mot. Res.) 22 (4), 255–268. https://doi.org/10.1080/08990220500420236.
Gibson, J.J., Radner, M., 1937. Adaptation, after-effect and contrast in the perception of tilted lines. I. Quantitative studies. J. Exp. Psychol. 20 (5), 453–467. https://doi.org/10.1037/h0059826.
Goudge, M.E., 1918. A qualitative and quantitative study of Weber's illusion. Am. J. Psychol. 29, 81. https://doi.org/10.2307/1414107.
Green, B.G., 1982. The perception of distance and location for dual tactile pressures. Percept. Psychophys. 31, 315–323. https://doi.org/10.3758/BF03202654.
Helson, H., 1930. The tau effect—An example of psychological relativity. Science 71, 536–537.
Hidaka, S., Tucciarelli, R., Azañón, E., Longo, M.R., 2020. Tactile distance adaptation aftereffects do not transfer to perceptual hand maps. Acta Psychol. 208, 103090. https://doi.org/10.1016/j.actpsy.2020.103090.
Hidaka, S., Tucciarelli, R., Azañón, E., Longo, M.R., 2022. Tilt adaptation aftereffects reveal fundamental perceptual characteristics of tactile orientation processing on the hand. J. Exp. Psychol. Hum. Percept. Perform. 48 (12), 1427–1438. https://doi.org/10.1037/xhp0001056.
Hidaka, S., Tucciarelli, R., Yusuf, S., Memmolo, F., Rajapakse, S., Azañón, E., Longo, M. R., 2024. Haptic touch modulates size adaptation aftereffects on the hand. J. Exp. Psychol. Hum. Percept. Perform. 50 (10), 989–999. https://doi.org/10.1037/xhp0001231.
Hong, S.W., Yoon, K.L., 2018. Intensity dependence in high-level facial expression adaptation aftereffect. Psychon. Bull. Rev. 25 (3), 1035–1042. https://doi.org/10.3758/s13423-017-1336-2.
Hsiao, S.S., Lane, J., Fitzgerald, P., 2002. Representation of orientation in the somatosensory system. Behav. Brain Res. 135 (1–2), 93–103. https://doi.org/10.1016/s0166-4328(02)00160-2.
Jeschke, M., Azañón, E., Drewing, K., 2025. Shared early processing of distinct tactile features. iScience 29 (2), 114485. https://doi.org/10.1016/j.isci.2025.114485.
Knight, F.L.C., Longo, M.R., Bremner, A.J., 2014. Categorical perception of tactile distance. Cognition 131 (2), 254–262. https://doi.org/10.1016/j.cognition.2014.01.005.
Li, L., Chan, A., Iqbal, S.M., Goldreich, D., 2017. An adaptation-induced repulsion illusion in tactile spatial perception. Front. Hum. Neurosci. 11, 331. https://doi.org/10.3389/fnhum.2017.00331.
Longo, M.R., 2017. Hand posture modulates perceived tactile distance. Sci. Rep. 7, 9665. https://doi.org/10.1038/s41598-017-08797-y.
Longo, M.R., 2020. Tactile distance anisotropy on the palm: a meta-analysis. Atten. Percept. Psychophys. 82, 2137–2146. https://doi.org/10.3758/s13414-019-01951-w.
Longo, M.R., 2022. Distortion of mental body representations. Trends Cognit. Sci. 26, 241–254. https://doi.org/10.1016/j.tics.2021.11.005.
Longo, M.R., 2025. The Invisible Hand: Neurocognitive Mechanisms of Human Hand Function. MIT Press.
Longo, M.R., Amoruso, E., Calzolari, E., Ben Yehuda, M., Haggard, P., Azañón, E., 2020. Anisotropies of tactile distance perception on the face. Atten. Percept. Psychophys. 82, 3636–3647. https://doi.org/10.3758/s13414-020-02079-y.
Longo, M.R., Ghosh, A., Yahya, T., 2015. Bilateral symmetry of distortions of tactile size perception. Perception 44 (11), 1251–1262. https://doi.org/10.1177/0301006615594949.
Longo, M.R., Golubova, O., 2017. Mapping the internal geometry of tactile space. J. Exp. Psychol. Hum. Percept. Perform. 43, 1815–1827. https://doi.org/10.1037/xhp0000434.
Longo, M.R., Haggard, P., 2011. Weber's illusion and body shape: anisotropy of tactile size perception on the hand. J. Exp. Psychol. Hum. Percept. Perform. 37, 720–726. https://doi.org/10.1037/a0021921.
Longo, M.R., Lulcuic, A., Sotakova, L., 2019. No evidence of tactile distance anisotropy on the belly. R. Soc. Open Sci. 6 (3), 180866. https://doi.org/10.1098/rsos.180866.
Mainka, T., Azañón, E., Zeuner, K.E., Knutzen, A., Bäumer, T., Neumann, W., Borngräber, F., Kühn, A.A., Longo, M.R., Ganos, C., 2021. Intact organization of tactile space perception in isolated focal dystonia. Mov. Disord. 36 (8), 1949–1955. https://doi.org/10.1002/mds.28607.
Manser-Smith, K., Tamè, L., Longo, M.R., 2021. Tactile distance anisotropy on the feet. Atten. Percept. Psychophys. 83, 3227–3239. https://doi.org/10.3758/s13414-021-02339-5.
Maravita, A., 1997. Implicit processing of somatosensory stimuli disclosed by a perceptual after-effect. Neuroreport 8 (7), 1671–1674. https://doi.org/10.1097/00001756-199705060-00022.
Martinelli, I., Risso, G., Bertoni, T., Meregalli, V., Collantoni, E., Molteni, F., Pedrocchi, A., Bottini, G., Serino, A., Bassolino, M., 2025. From adolescence to old age: how sensory precision shapes body ownership during physiological aging. Front. Hum. Neurosci. 19, 1663505. https://doi.org/10.3389/fnhum.2025.1663505.
Miller, L.E., Longo, M.R., Saygin, A.P., 2016. Mental body representations retain homuncular shape distortions: evidence from Weber's illusion. Conscious. Cognit. 40, 17–25. https://doi.org/10.1016/j.concog.2015.12.008.
Oldfield, R.C., 1971. The assessment and analysis of handedness: the Edinburgh inventory. Neuropsychologia 9, 97–113. https://doi.org/10.1016/0028-3932(71)90067-4.
Pond, S., Kloth, N., McKone, E., Jeffery, L., Irons, J., Rhodes, G., 2013. Aftereffects support opponent coding of face gender. J. Vis. 13 (14), 16. https://doi.org/10.1167/13.14.16.
Pubols, L.M., Leroy, R.F., 1977. Orientation detectors in the primary somatosensory neocortex of the raccoon. Brain Res. 129, 61–74. https://doi.org/10.1016/0006-8993(77)90970-2.
Reid, E., Harvie, D., Miegel, R., Spence, C., Moseley, G.L., 2015. Spatial summation of pain in humans investigated using transcutaneous electrical stimulation. J. Pain 16 (1), 11–18. https://doi.org/10.1016/j.jpain.2014.10.001.
Rhodes, G., Jeffery, L., 2006. Adaptive norm-based coding of facial identity. Vis. Res. 46 (18), 2977–2987. https://doi.org/10.1016/j.visres.2006.03.002.
Rhodes, G., Pond, S., Jeffery, L., Benton, C.P., Skinner, A.L., Burton, N., 2017. Aftereffects support opponent coding of expression. J. Exp. Psychol. Hum. Percept. Perform. 43 (3), 619–628. https://doi.org/10.1037/xhp0000322.
Robbins, R., McKone, E., Edwards, M., 2007. Aftereffects for face attributes with different natural variability: adapter position effects and neural models. J. Exp. Psychol. Hum. Percept. Perform. 33 (3), 570–592. https://doi.org/10.1037/0096-1523.33.3.570.
Silver, R.J., 1969. Tilt after-effects in Touch. Brandeis University. Unpublished PhD dissertation.
Solomon, S.G., Kohn, A., 2014. Moving sensory adaptation beyond suppressive effects in single neurons. Curr. Biol. 24 (20), R1012–R1022. https://doi.org/10.1016/j.cub.2014.09.001.
Stone, K.D., Keizer, A., Dijkerman, H.C., 2018. The influence of vision, touch, and proprioception on body representation of the lower limbs. Acta Psychol. 185, 22–32. https://doi.org/10.1016/j.actpsy.2018.01.007.
Tamè, L., Khan, N., Allarakhia, K., Longo, M.R., Azañon, E., 2026. Tactile adaptation transfers between distance and continuous size. Proceedings of the Royal Society B 293, 20252678. https://doi.org/10.1098/rspb.2025.2678.
Taylor-Clarke, M., Jacobsen, P., Haggard, P., 2004. Keeping the world a constant size: object constancy in human touch. Nat. Neurosci. 7, 219–220. https://doi.org/10.1038/nn1199.
Thakur, P.H., Fitzgerald, P.J., Lane, J.W., Hsiao, S.S., 2006. Receptive field properties of the macaque second somatosensory cortex: nonlinear mechanisms underlying the representation of orientation within a finger pad. J. Neurosci. 26 (52), 13567–13575. https://doi.org/10.1523/JNEUROSCI.3990-06.2006.
Tosi, G., Romano, D., 2020. The longer the reference, the shorter the legs: how response modality affects body perception. Atten. Percept. Psychophys. 82 (7), 3737–3749. https://doi.org/10.3758/s13414-020-02074-3.
Uccelli, S., Pisu, V., Riggio, L., Bruno, N., 2019. The Uznadze illusion reveals similar effects of relative size on perception and action. Exp. Brain Res. 237 (4), 953–965. https://doi.org/10.1007/s00221-019-05480-8.
Uznadze, D.N., 1966. The Psychology of Set. Consultants Bureau.
van der Horst, B.J., Duijndam, M.J.A., Ketels, M.F.M., Wilbers, M.T.J.M., Zwijsen, S.A., Kappers, A.M.L., 2008a. Intramanual and intermanual transfer of the curvature aftereffect. Exp. Brain Res. 187 (3), 491–496. https://doi.org/10.1007/s00221-008-1390-0.
van der Horst, B.J., Willebrands, W.P., Kappers, A.M.L., 2008b. Transfer of the curvature aftereffect in dynamic touch. Neuropsychologia 46 (12), 2966–2972. https://doi.org/10.1016/j.neuropsychologia.2008.06.003.
Weber, E.H., 1834. De subtilitate tactus (H. E. Ross, Trans.). In: E. H. Weber on the Tactile Senses, second ed. Academic Press, pp. 21–128.
Webster, M.A., Leonard, D., 2008. Adaptation and perceptual norms in color vision. J. Opt. Soc. Am. A 25 (11), 2817–2825. https://doi.org/10.1364/josaa.25.002817.